Spatiotemporal Quantification of Organic Matter Accumulation in the Eocene Green River Formation, Bridger Basin, Wyoming



Marshal Tofte¹ and Alan R. Carroll²

- ¹Madison, Wisconsin, marshal_tofte@hotmail.com
- ²Department of Geoscience, University of Wisconsin-Madison, Madison, Wisconsin

ABSTRACT

It has long been recognized that lakes can bury large amounts of organic carbon (C_{ORG}) in their sediment, with important consequences for conventional and unconventional petroleum resources and potentially for the global carbon cycle. The detailed distribution of lacustrine organic carbon through space and time is important to understanding its commercial and climatic implications, but has seldom been documented in detail. The Green River Formation offers a unique opportunity to improve this understanding, due to extensive Fischer assay analyses of its oil generative potential and to recently published radioisotopic age analyses of intercalated volcanic tuffs. Fischer assay analyses reveal distinctly different patterns of organic matter enrichment that correlate with different lacustrine facies associations. Histograms of oil generative potential for evaporative facies of the Wilkins Peak Member exhibit an approximately exponential distribution. This pattern is interpreted to result from episodic expansion and contraction of Eocene Lake Gosiute across a low-gradient basin floor that experienced frequent desiccation. In contrast, histograms for fluctuating profundal facies of the upper Rife Bed of the Tipton Member and the lower LaClede Bed of the Laney Member exhibit an approximately normal or log normal distribution, with modes as high as 16–18 gallons per ton. This pattern is interpreted to reflect generally deeper conditions when the lake often intersected basin-bounding uplifts. Within the Bridger basin, burial of C_{ORG} was greatest in the south during initial Wilkins Peak Member deposition, reflecting greater rates of accommodation near the Uinta uplift. The locus of C_{ORG} burial shifted north during upper Wilkins Peak Member deposition, coincident with a decrease in differential accommodation. C_{ORG} burial during deposition of the upper Rife and lower LaClede Beds was greatest in the southeast, due either to greater accommodation or localized influx of river-borne nutrients. Average C_{ORG} burial fluxes are consistently ~4-5 g/m²yr for each interval, which is an order of magnitude less than fluxes reported for small Holocene lakes in the northern hemisphere. Maximum rates of C_{ORG} burial during deposition of organic-rich mudstone beds (oil shale) were likely similar to Holocene lakes however. Deposition of carbonate minerals in the Bridger basin resulted in additional, inorganic carbon burial. Overall it appears that carbon burial by Eocene lakes could have influenced the global carbon cycle, but only if synchronized across multiple lake systems.

INTRODUCTION

Lakes function both as major organic carbon (C_{ORG}) sinks and as sources of CO₂ and CH₄ emissions to the atmosphere (e.g., Cole and others, 2007; Duarte and others, 2007; Tranvik and others, 2009). Despite covering only a small fraction of the continents (\sim 3%; Downing and others 2006) they represent a disproportionately important component of the global carbon cycle. Based on analysis of late Holocene sediment from small lakes in Minnesota and from Lake Michigan, Dean and Gorham (1998) estimated that freshwater lakes bury C_{ORG} at an average rate of ~42 Tg/yr, compared to ~100 Tg/yr for the ocean. The magnitude and impact of C_{ORG} (organic carbon) burial by older lakes is largely unknown, but may have been similarly large. Ancient lacustrine mudstone commonly reaches or exceeds 20% total organic carbon (%TOC; e.g., Horsfield and others, 1994; Carroll and Bohacs, 2001; Carroll and Wartes, 2003). Lacustrine organic-rich rocks source many conventional petroleum accumulations, particularly in east and southeast Asia and in the South Atlantic region, and include vast oil shale deposits. Oil shale in the Eocene Green River Formation in the western U.S. alone has been assessed at ~4.3 trillion barrels of oil in place (Johnson and others, 2011), an amount that greatly exceeds estimated global reserves of recoverable conventional oil. It is unclear how much of this total could be economically produced, but even at low recovery rates it would remain a substantial resource. On the other hand, the combustion of oil from oil shale could add significantly to the release of CO₂ to the atmosphere. Disregarding emissions related to extraction and retorting, combustion of 4.3 trillion barrels of oil would release roughly 1930 Gt of CO₂

(Hood and Cole, 2015). This is equivalent to ~55 years of anthropogenic emissions at present rates.

Hood and Cole (2015) calculated that burial of all the C_{ORG} in the Green River Formation would have reduced atmospheric CO₂ concentration by 377 ppm, and suggested that such burial might have contributed to a reversal of warming during the Early Eocene Climatic Optimum. They did not take into account feedbacks such as carbon storage in the terrestrial biosphere, oceanic absorption of CO₂, and silicate weathering however (e.g., Archer, 2005), that might have reduced the impact of carbon burial on atmospheric CO₂ concentration. Considered over the ~8 my of Green River Formation deposition, average annual C_{ORG} burial in the Green River Formation would likely have been minor in comparison to other fluxes in the global carbon cycle.

How then can this observation be reconciled with the conclusion of Dean and Gorham (1998) and Tranvik and others (2009) that lakes do play an important role? Resolution of this paradox first requires an accurate understanding of the spatial and temporal patterns of C_{ORG} in lacustrine strata, which is challenging to obtain. Mudstone is well known for its heterogenous organic matter distribution at multiple scales (e.g., Macquaker and Howell, 1999; Passey and others, 2010). %TOC measurements made from small, isolated samples are seldom adequate for a truly quantitative assessment of C_{ORG} content. Additionally, the determination of C_{ORG} burial rates also requires detailed knowledge of net rock accumulation rates. This information is readily accessible in Holocene sediment via counting of annual laminations (varves) and radiocarbon dating. It is notoriously difficult to obtain in many pre-Quaternary lake deposits, however. Biostratigraphy is often limited to relatively wide-ranging, endemic taxa, and radioisotopic dating requires the availability of suitable volcanic tephras. The problem of determining accurate C_{ORG} burial rates may be exacerbated if lacustrine facies associations changed through time (cf. Carroll and Bohacs, 1999; Bohacs and others, 2000), or if the relative rate of inorganic sediment input varied (Bohacs and others, 2005). Finally, estimating the magnitude of global carbon burial by lakes depends on knowing their global distribution and size. Compilations of pre-Quaternary lakes at specific moments in geologic time are often limited by incomplete preservation or by lack of recognition of lake deposits. Notably, most of the small late Holocene lakes included in Dean and Gorham's study are geologically ephemeral, fated to eventual erasure by the next advance of continental ice sheets, and will therefore leave little record of themselves in future eras. Paleogeographic reconstructions of pre-Quaternary lakes generally rely on

approximate age estimates (e.g., Carroll and others, 2010), making it difficult or impossible to determine if organic matter burial in different lakes occurred synchronously.

The Green River Formation in the Bridger basin in Wyoming is well suited to addressing these problems for two main reasons. First, hundreds of exploratory wells have been drilled in order to assess its oil shale potential (Figure 1). Samples from these wells were analyzed via Fischer assay, which unlike %TOC provides a truly complete, quantitative measurement of organic matter enrichment (expressed in gallons of oil per ton, GPT). Previous U.S Geological Survey

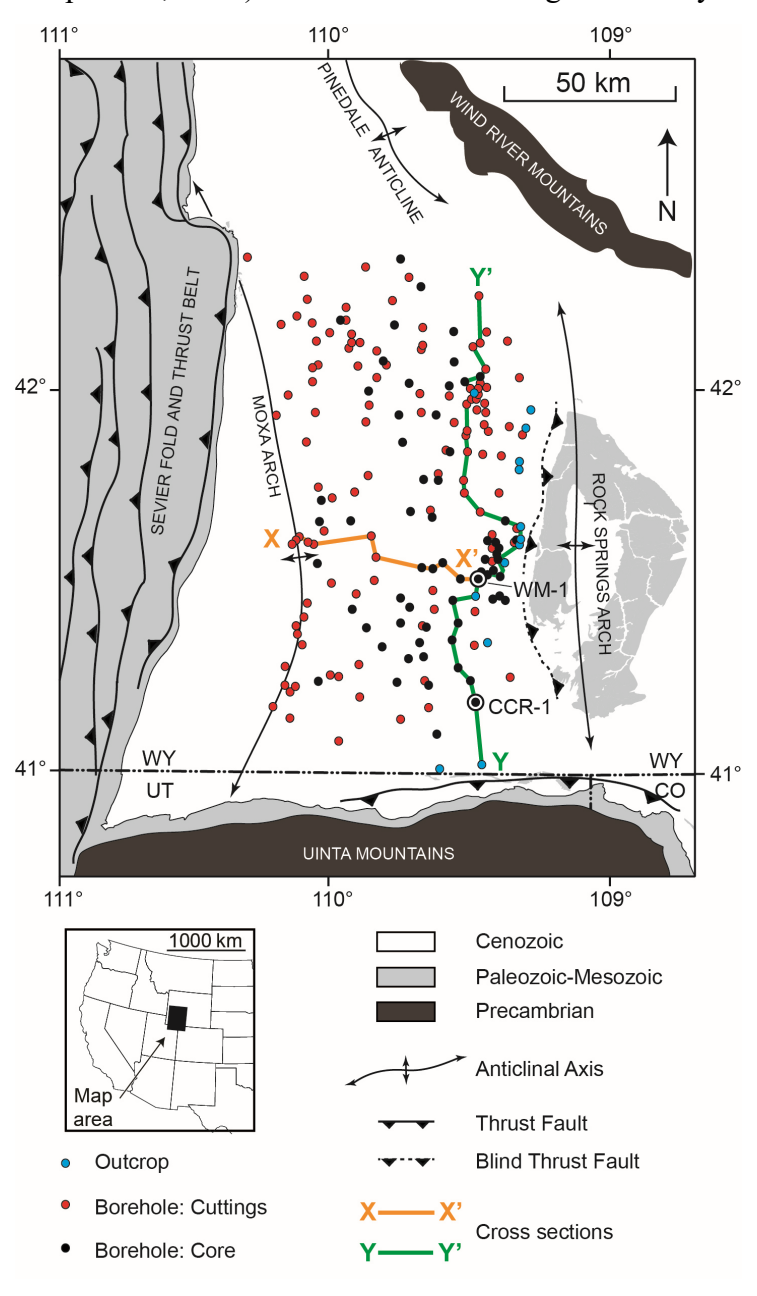


Figure 1. Geologic setting and location of outcrop sections and of cores with Fischer assay data (modified from Johnson and others, 2011). WM-1 = White Moutain #1 core; CCR-1 = Currant Creek Ridge #1 core.

work has already provided an exhaustive regional synthesis of these data (Johnson and others, 2011). Second, radioisotopic dating of intercalated tuffs has provided a geochronologic framework that is perhaps unique in its accuracy and resolution (Figure 2). In this study we combine a reinterpreted stratigraphic

analysis of Fischer Asssay data with detailed chronostratigraphy based on recent tuff dating (Smith and others, 2010; Machlus and others, 2015). The result is a comprehensive analysis of spatially and temporally varying C_{ORG} burial rates for a key part of the Green River Formation, focused on 4 discrete time intervals.

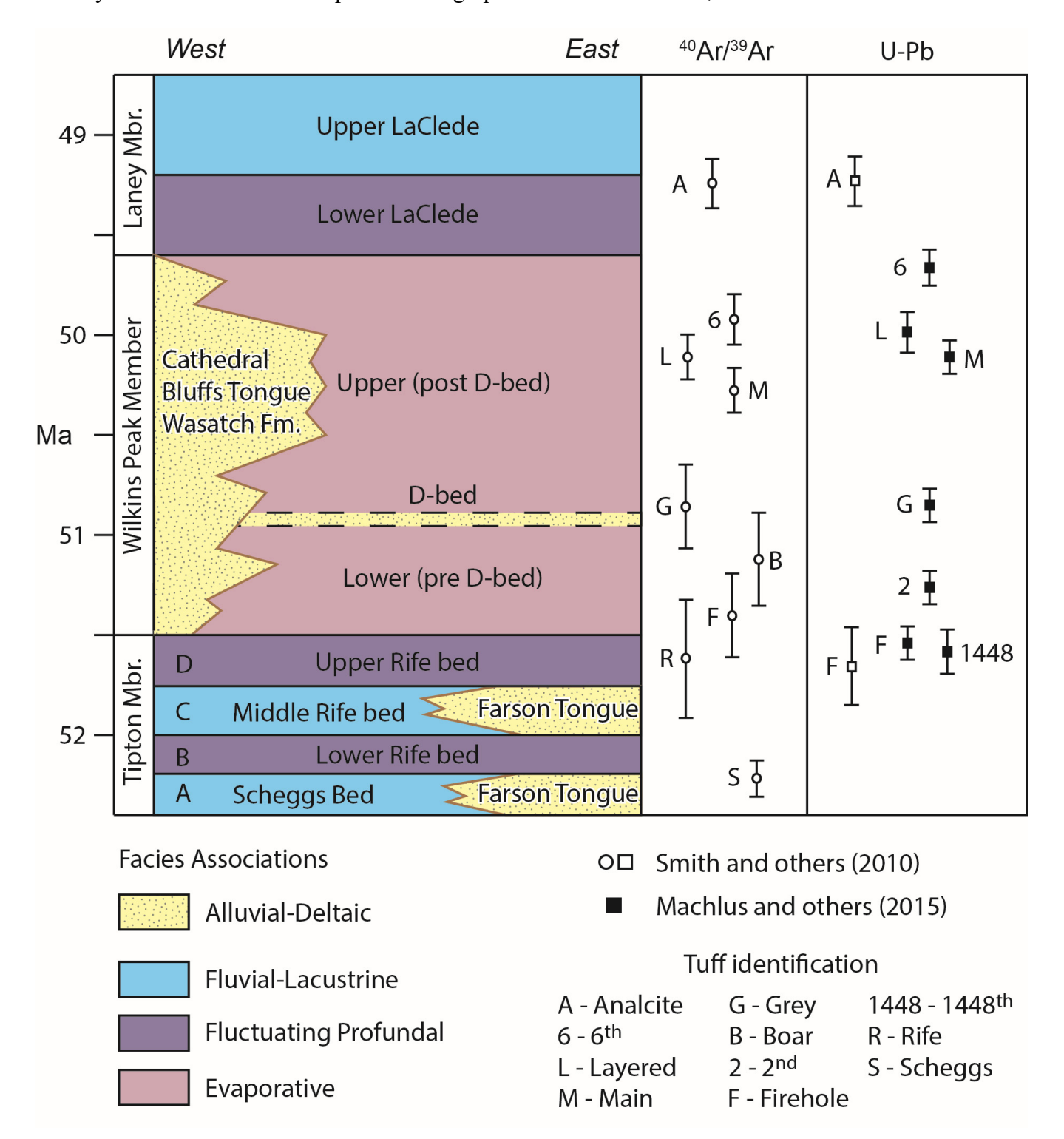


Figure 2. Chronostratigraphy of the Green River Formation in the Bridger basin, based on radiosotopic ages reported by Smith and others (2010) and Machlus and others (2015). Bars indicate $\pm 2\sigma$ error ranges.

SETTING

Lake Gosiute occupied the greater Green River Basin during deposition of the Green River Formation from ~53.5–48.5 Ma (Bradley, 1964; Smith and others, 2010; Machlus and others, 2015). This composite basin was bounded by the Sevier fold and thrust belt to the west and by the several Precambrian-cored uplifts to the south, east, and north (Love, 1960; Dickinson and others, 1988; Figure 1). It is internally partitioned by several lower-relief structures including the Rock Springs arch, which exposes upper Cretaceous rocks at its core and separates the Bridger Basin to the west from the Great Divide, Washakie, and Sand Wash basins to the east. This study focuses on the Bridger Basin due to the relatively complete record of lacustrine deposition available there.

The Green River Formation consists of predominantly lacustrine deposits and reaches 750+ meters in thickness in the southern Bridger Basin (Roehler, 1992). It is underlain by and laterally transitional with the alluvial Wasatch Formation. The Green River Formation contains a wide range of sedimentary facies, which Carroll and Bohacs (1999) classified as belonging to fluvial-lacustrine, fluctuating profundal, and evaporative facies associations. The fluviallacustrine association is interpreted to reflect deposition in hydrologically-open, freshwater lakes, and is characterized by lateral heterogeneity, molluscan and other fossils, and mixed terrestrial and aquatic organic matter (Carroll and Bohacs, 2001). Its stratigraphic architecture is strongly influenced by shoreline progradation within an overfilled lake basin (Bohacs and others, 2000). The fluctuating profundal facies association generally lacks molluses, suggesting brackish to saline conditions, but fish fossils are common. Organic matter consists dominantly of amorphous kerogen, inferred to derive from algae and cyanobacterial sources, with only minor input of terrestrial organic matter (vitrinite and inertinite; Horsfield and others, 1994). Stratigraphic successions record a combination of progradational and aggradational architecture, produced by lakes that alternated between open and closed hydrology within a balanced-fill lake basin. Finally, the evaporative facies association is distinguished by the preservation of lacustrine evaporite (including Na-carbonate) and the absence of aquatic macrofaunal fossils. Its organic matter is predominantly amorphous, and it forms repetitive, aggradational lake expansion-contraction cycles that extend across much of the underfilled lake basin in which they were deposited.

Smith and others (2008) noted that lacustrine facies evolve progressively from the fluvial lacustrine as-

sociation (Luman Tongue and Scheggs Bed of the Tipton Member), to fluctuating profundal facies (the Rife Bed of the Tipton Member), to evaporative facies (the Wilkins Peak Member), then back again through fluctuating profundal (the lower LaClede Bed of the Laney Member), and finally to fluviallacustrine (the upper LaClede Bed; Figure 2). Later work has revealed a more complex history for the Tipton Member, featuring two intervals of fluviallacustrine facies (zones A and C) and two of fluctuating profundal facies (zones B and D, Graf and others, 2015; Figure 2). The contacts between facies associations are generally conformable but abrupt, marking wholesale changes in paleolimnology and sedimentation patterns. Carroll (2017) proposed the new term xenoconformity to describe such contacts, in recognition that the successions on either side of the contacts do not conform to Walther's Law (cf. Middleton, 1973).

The present study focuses on the upper Rife Bed of the Tipton Member, the Wilkins Peak Member, and the lower LaClede Bed of the Laney Member. The upper Rife Bed consists of variably organic-rich mudstone and fossil-bearing siltstone with minor occurrences of ostracode and oolitic grainstone and local stromatolite. It also contains fish fossils. It is characterized by generally dolomitic mineralogy and elevated $\delta^{18}O$ and $\delta^{13}C$ values relative to underlying fluvial-lacustrine facies, suggesting enhanced evaporation. The top of the upper Rife bed makes an abrupt contact with the Wilkins Peak Member, referred to by Pietras and Carroll (2006) as a sequence boundary. Erosion of this surface appears to be minor however, and we reinterpret it herein as a xenoconformity.

The Wilkins Peak Member is composed predominantly of light gray, dolomitic to calcitic marlstone, with lesser amounts of organic-rich marlstone (oil shale), thin calcareous sandstone beds, bedded trona and halite, and displacive shortite (Bradley and Eugster, 1969; Smoot, 1983; Pietras and Carroll, 2006; Jagniecki and Lowenstein, 2015). These lacustrine facies alternate with up to nine composite bedsets containing fine-grained fluvial facies (named marker beds A through I by Culbertson 1961; Pietras and Carroll, 2006; Figures 3, 4). These recur on a ~100 ky interval corresponding to short eccentricity (Aswasereelert and others, 2013; Smith and others, 2014). Most of the bedded evaporite occurs in the lower Wilkins Peak Member below the C marker bed (Smith and others, 2008). Calcite content of marlstone increases above the D marker bed (Mason, 2012), resulting in a prominent "white band." In recognition of these changes the present study subdivides the Wilkins Peak Member informally into lower

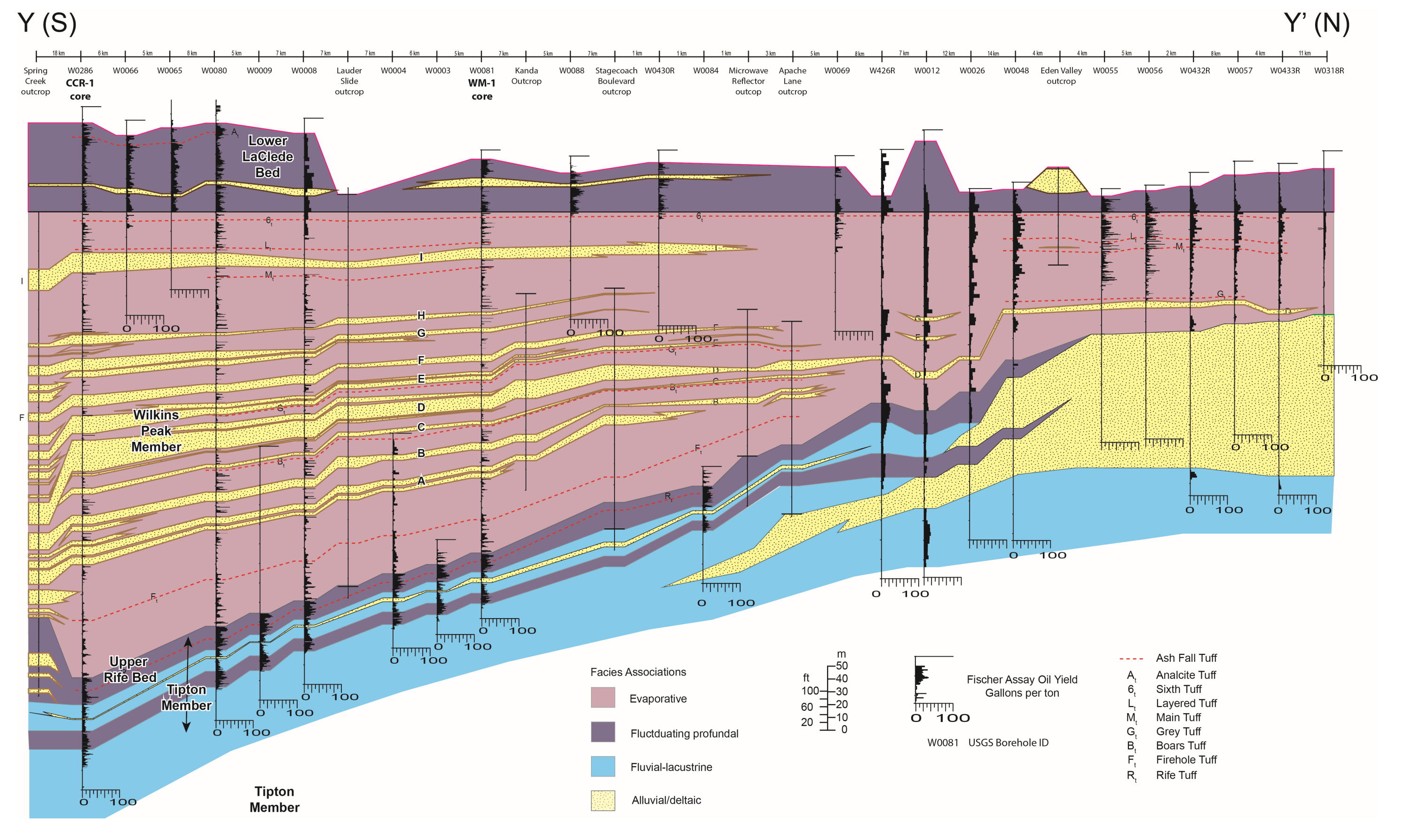
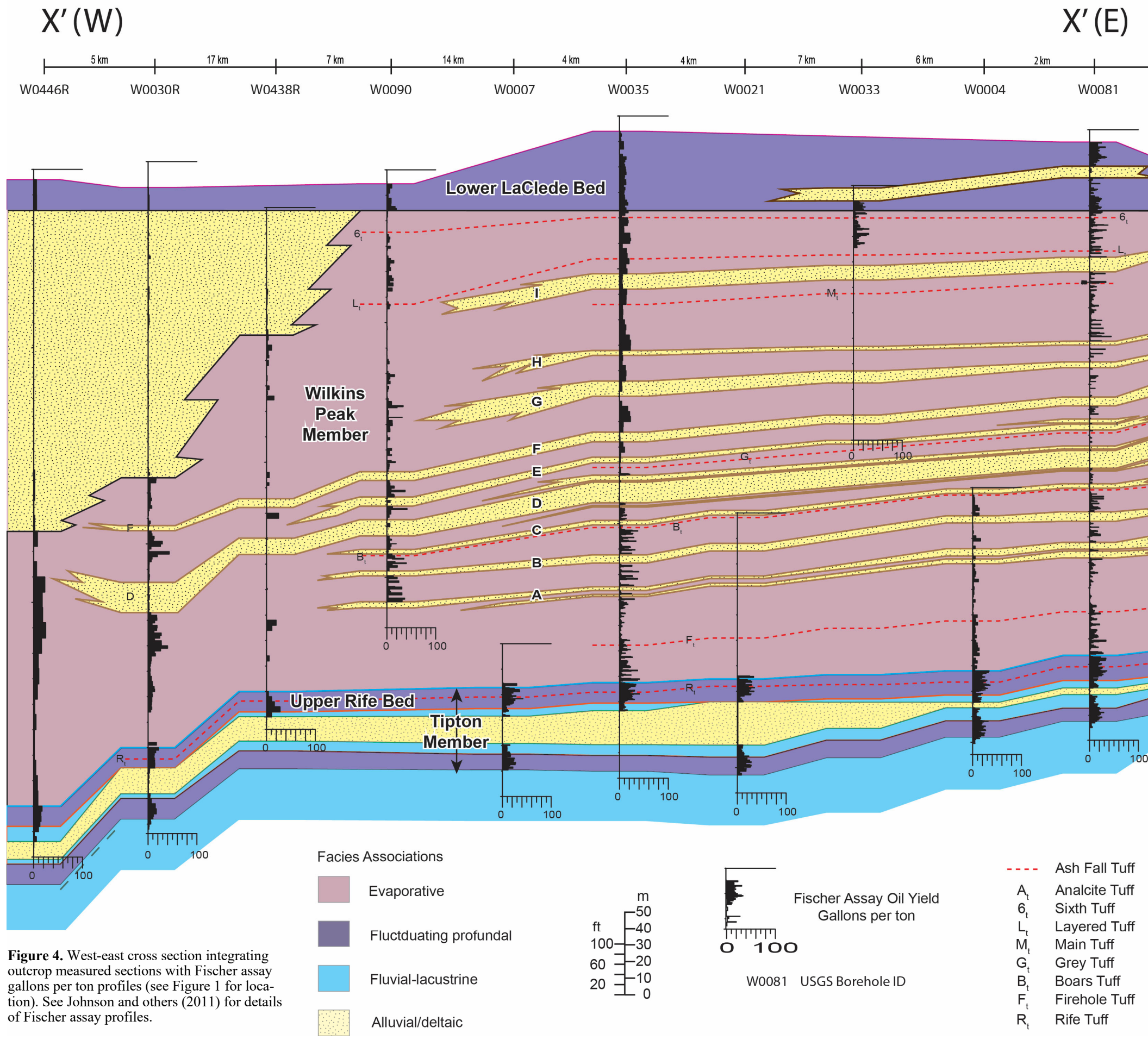


Figure 3. South-north cross section integrating outcrop measured sections with Fischer assay gallons per ton profiles (see Figure 1 for location). See Johnson and others (2011) for details of Fischer assay profiles and Pietras and Carroll (2006) and Smith and others (2015) for details of outcrop sections.



and upper parts, demarcated by the top of the D-bed.

The upper contact of the Wilkins Peak Member marks another abrupt transition into fluctuating profundal facies of the lower LaClede Bed. Due to its conformable nature and the non-Waltherian nature of the facies successions below and above, Carroll (2017) interpreted this surface as a xenoconformity. The lower LaClede bed is composed principally of organic-rich laminated marlstone (Bradley, 1964) while lesser amounts of dolomitic marlstone and tuffaceous siltstone and sandstone are also present (Roehler, 1992; Surdam and Stanley, 1979; Rhodes and Carroll, 2015). It also marks the sudden reappearance fish bones and other macrofossils after an absence of nearly 2 my.

METHODS

The study is based on three main parts: construction of a chronostratigraphic age model, conversion of Fischer assay oil yields to %TOC, and calculation and mapping of net C_{ORG} and C_{INORG} burial rates.

Chronostratigraphy

Green River Formation stratigraphic units were mapped on the basis of Fischer assay histograms made available by the U.S. Geological Survey (Johnson and others, 2011), supplemented by visual descriptions of selected drill cores (Figure 1). This approach assumes that individual oil shale beds represent major expansions of Lake Gosiute that were synchronous or nearly so across the Bridger basin, an assumption that is supported by their close parallelism with distinctive tuff beds (Smith and others, 2008; 2015; Figures 3, 4). One limitation of Fischer assay data is that the stratigraphy they establish generally stops short of the basin margins, due to gradual lateral transitions from lacustrine to alluvial facies. Fischer assay and %TOC analyses indicate negligible organic matter in the alluvial facies.

The upper Rife bed of the Tipton Member as used in this study is limited to the uppermost interval of fluctuating profundal facies (Tipton zone D of Graf and others, 2015), in order to ensure that the results represent a single facies association. It does not conform with the more inclusive Rife Bed interval evaluated by the United States Geological Survey (Johnson and others, 2011), which also incorporated underlying fluvial-lacustrine facies. Fluvial-lacustrine facies were excluded from mapping in this study due to the greater difficulty of determining chronostratigraphic correlations in these laterally discontinuous deposits. The lower LaClede bed was interpreted as an amal-

gamation of the intervals designated by Johnson and others (2011) as the "rich LaClede bed," "lower rich LaClede bed," and the "lower lean LaClede bed." The lower LaClede Bed corresponds to the fluctuating profundal facies association, and excludes the overlying fluvial lacustrine facies of the upper LaClede Bed. The chronology used in this study is based on ⁴⁰Ar/³⁹Ar and U-Pb ages for 9 tuff horizons (Figure 2; Smith and others, 2010; Machlus and others, 2015), based on their positions in the Currant Creek Ridge 1 core (CCR-1, Figure 1). Linear interpolation between tuff beds was used to estimate the age of contacts between the stratigraphic units in this study (Table 1).

Table 1. Radioisotopic Ages of Stratigraphic Boundaries.

Boundary	Estimated Age (Ma)
Top lower LaClede Bed	49.2
Top Wilkins Peak Member	49.6
Top of D-bed	50.9
Top of upper Rife Bed	51.5
Base of upper Rife Bed	51.8

Conversion of Fischer Assay Data to %TOC

Fischer and Schrader (1920) originally developed the Fischer assay (FA) method for application to coal retorting, and later adapted by Stanfield and Frost (1949) for oil shale assay. Procedural methods (e.g., maximum retort temperature, duration of incremental heating periods, or the grain size of the sample post-powdering and homogenization) can greatly affect the results attained (Goodfellow and Atwood, 1974; Heistand, 1976; Keighin, 1980). The Fischer assay method was standardized from 1984–1996 within ASTM D3904 (see Johnson and others, 1984, for a full description of Fischer assay methods and limitations applicable of Bridger basin samples).

Fischer assay and TOC integrate sample material over different depth scales, representing a key difference in how these two parameters express organic matter content. Samples for Fischer assay are combined and homogenized over intervals ranging from ~30–300 cm, in order to obtain a true quantitative measure of oil generation potential (Figure 5). In contrast, %TOC analysis requires only a few hundred mg of powdered rock and typically reflects ~1–10 mm vertical resolution, but most of the core volume is not sampled. Direct sample-to-sample comparison of these data sets therefore is not possible, but averaged comparisons of samples representing larger intervals

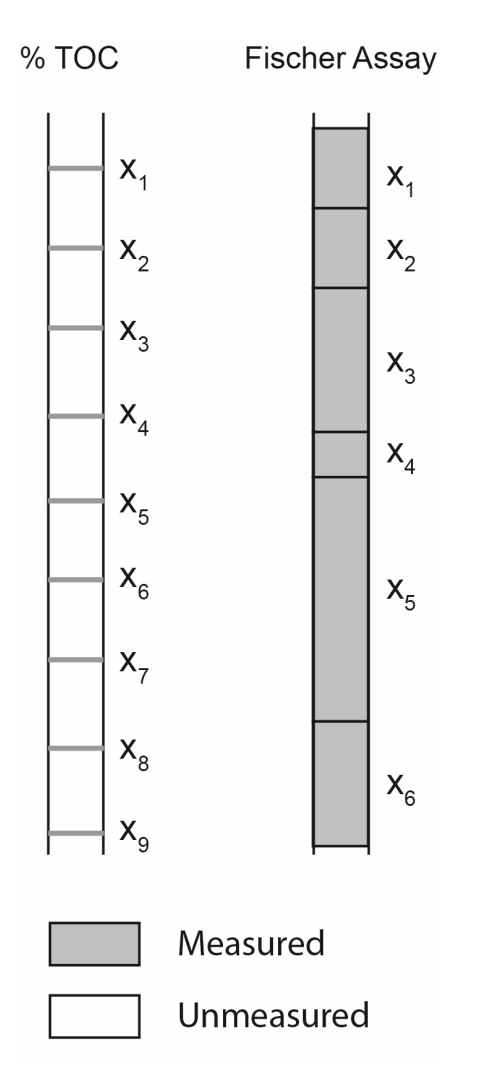


Figure 5. Comparison of sampling methodologies used for %TOC versus Fischer assay analyses.

can provide an accurate calibration. A relationship of Fischer assay gallons per ton and %TOC of the present study was achieved using previously published Fischer assay data (Johnson and others, 2011) and previously published %TOC data for the Wilkins Peak Member (Carroll and Bohacs, 2001; U.S.G.S. Core Research Center), combined with new %TOC data obtained from the Tipton Member in the WM-1 core (Figure 1). New %TOC samples were selected at ~30 cm spacing, excluding sandstone intervals, and samples were powdered and homogenized using a steel ball mill. Weatherford Labs employed a LECO C230 Carbon Analyzer for %TOC analyses. Linear regression of Fischer assay gallons per ton (GPT) versus %TOC results in a closely similar relationship for each of the three study units (Figure 6). We therefore use the simplified formula %TOC = 0.4 \$GPT + 1 to convert all Fischer assay values in this study to % TOC. This formula is similar to previously reported relationships (Smith, 1966; Cook, 1974; and Heistand and Humphries, 1976). The variance in Figure 6 is at least partly attributable to the dissimilar sampling

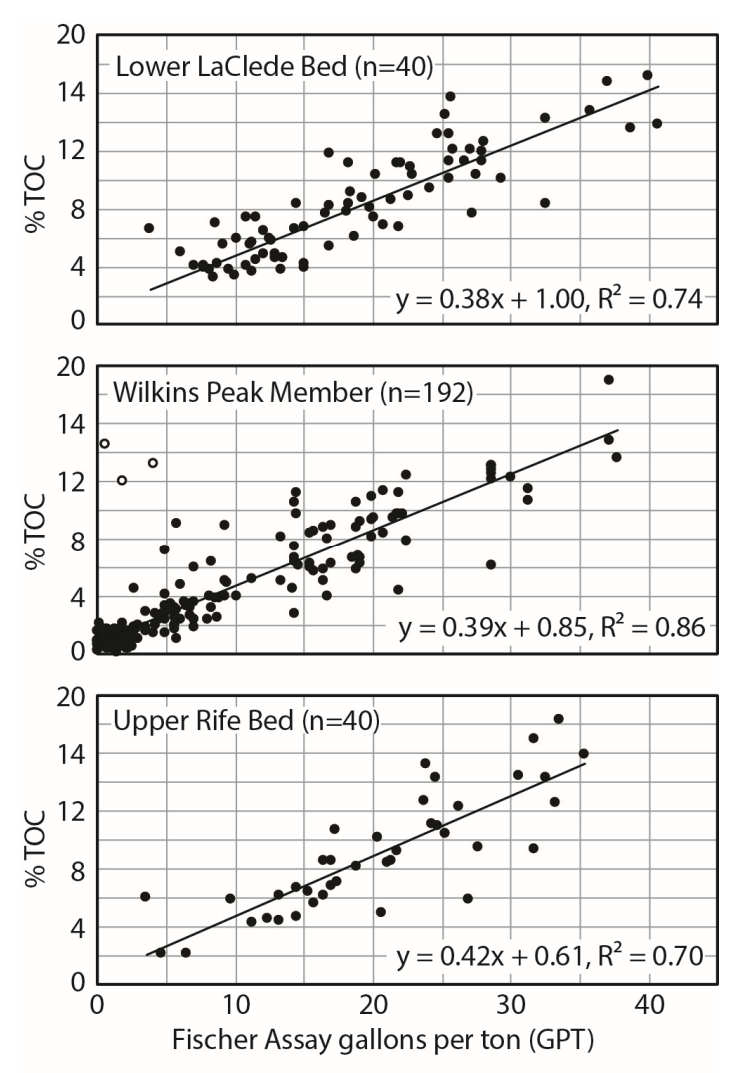


Figure 6. Comparison of Fischer assay gallons per ton to %TOC measured for the same samples.

stratgies used for each type of analysis, but it could also partly reflect differences in organic matter type. Similar relationships are found for both fluctuating profundal (upper Rife Bed, lower LaClede Bed) and evaporative (Wilkins Peak Member) facies associations.

C_{ORG} Burial Rates

C_{ORG} mass and net mass accumulation rates for each of the four study intervals were calculated based on thickness-weighted average %TOC at each core site (derived from Fischer assay) and an assumed average rock density of 2500 kg/m³ for simplicity. Measurements of actual rock density of the study samples were not available, but are not critical to the results. Contour maps were created for each study interval using the contour tool within QGIS (2014). Only data from cored intervals were used in mapping, and the mapping boundaries vary based on the distribution of lacustrine vs alluvial facies within each interval. Total C_{ORG} burial for each interval (Table 2)

Table 2. Net Carbon Burial (Gt=gigatons)

Unit	C _{ORG} (Gt)	C _{INORG} (Gt)	F _{ORG} (%)
Lower Laclede Bed	16.7	24.2	40.8
Wilkins Peak Member (post-D)	46.1	62.5	42.4
Wilkins Peak Member (pre-D)	18.6	42.3	30.6
Upper Rife Bed	10.6	9.5	52.7

was determined by integration of the contour maps. The calculated magnitudes of C_{ORG} burial obtained in this study are broadly compatible the Fischer results obtained by Johnson and other (2011), despite the different methodologies employed. For example, Johnson and others (2011) reported a potential generation of 704,991 barrels of oil in the Wilkins Peak Member, the equivalent of ~80 Gt of C_{ORG} (assuming 7.5 barrels per ton oil and 85% by carbon by weight). In this study C_{ORG} burial in the same interval is estimated at 65 Gt.

CINORG Burial Rates

C_{INORG} values were calculated based on the assumption that calcite and dolomite together average 50% of Green River Formation inorganic constituents. Actual values determined vary widely, between ~20–80% based on XRD peak heights (Mason, 2012; Graf and others, 2015). However, insufficient data are available for the core samples to further refine estimates of C_{INORG}.

RESULTS

Fischer Assay Stratigraphy

Fischer assay profiles permit reliable basin-scale correlation of the four stratigraphic intervals included in this study. The lower boundary of the upper Rife bed is marked by a consistent increase in GPT relative to the underlying fluvial-lacustrine facies (Figures 3 and 4). A general decrease in the frequency of organic-rich beds occurs in the lowermost Wilkins Peak Member. Its internal stratigraphy is delineated by the repetitive occurrence of sandstone marker beds A-I, which are identifiable as gaps in the otherwise continuous Fischer assay profiles. The D bed, used to subdivide lower and upper units of the Wilkins Peak Member, is readily correlable across the basin. The upper contact of the Wilkins Peak Member is marked by an abrupt increase in the frequency of organic-rich beds in the lower LaClede Bed. The upper LaClede Bed is mostly missing from the Fischer assay histograms, either because it is absent or because it was not sampled for analysis. Doebbert and others (2010) noted that it is in fact present in some outcrops in the southern Bridger basin, but that it transitions laterally into sandstone facies of the Sand Butte Bed in the northern half of the basin.

The Wilkins Peak Member thickens by a factor of about 3 times from north to south, with the greatest thickening occurring within the pre-D bed interval (Figure 3). The upper Rife Bed and lower LaClede Bed are more uniform in thickness across the basin, although the upper Rife Bed either pinches out or grades laterally into flood plain facies near the northern basin margin (Graf and others, 2015; Figure 3). The upper half of the Wilkins Peak Member grades laterally into alluvial siliciclastic sandstone facies in the western Bridger basin (Figure 4). No Fischer assay analyses are reported for the area west of the Moxa arch (Figure 1).

Fischer assay GPT Frequency Distributions

Histograms displaying the frequency distribution of Fischer assay GPT manifest two distinctly different patterns that correspond to different facies associations (Figure 7). Fluctuating profundal facies (upper Rife Bed, lower LaClede Bed) approximate a normal or lognormal distribution, whereas evaporative facies (Wilkins Peak Member) approximate an exponential distribution. The upper Rife Bed is the most organicrich interval, with a modal value of 16–18 GPT and a mean value of ~19 GPT. The distribution for the lower LaClede Bed is similar in shape but shifted to the right. Modal and mean values are 7–11 GPT and ~12 GPT respectively. In contrast, the modal value for the Wilkins Peak Member is 1–2 GPT and the mean is \sim 8 −10 GPT. Note however that Figure 7 excludes samples with <0.5 GPT for consistency and for clarity of presentation; the modal values for the Wilkins Peak Member would be 0-1 GPT if all samples were included, and the mean GPT would be reduced. It must also be noted that the histograms incorporate samples of unequal thickness; thickness-weighted means are ~2 GPT lower for the upper Rife and lower LaClede beds and ~1 GPT lower for the Wilkin's Peak Member. Maximum oil generative potential is similar for all 4 units. Finally, it is noteworthy that despite the generally leaner character of the Wilkins Peak Member, its total C_{ORG} content is more than twice that of the other two intervals combined (Table 2).

Geographic Patterns of Organic Enrichment

Figure 8 summarizes the geographic evolution of the four study intervals in the Bridger Basin, based on interval thickness, C_{ORG} burial, average %TOC, and C_{ORG} burial rates. The most obvious thickness pattern

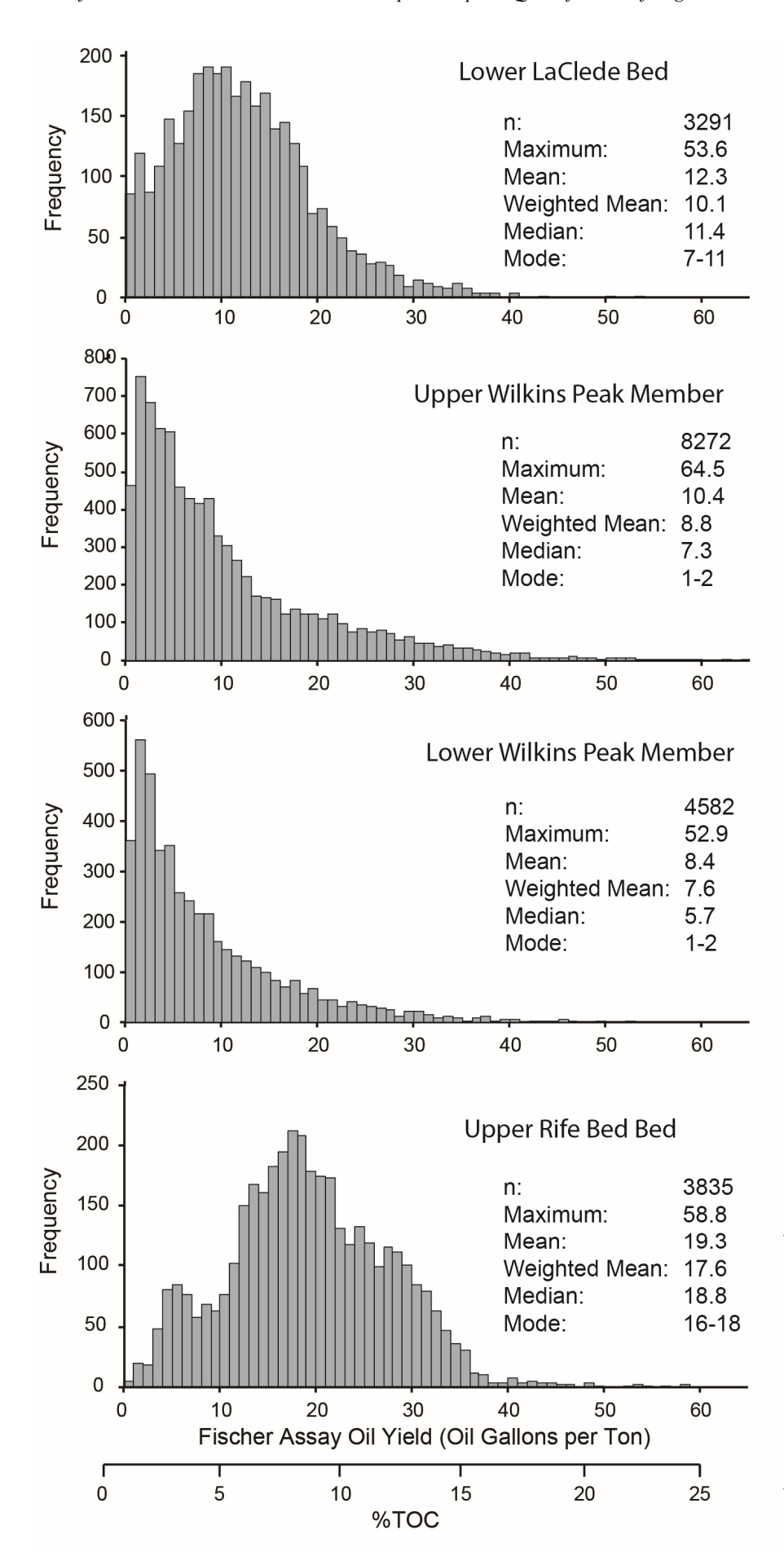


Figure 7. Basinwide Fischer assay oil yield frequency distribution histograms for four study intervals. Note that the Rife Bed and Wilkins Peak analyses are based solely on the Bridger Basin, whereas the LaClede Bed plot also includes samples from the Washakie Basin in order to obtain comparable numbers of analyses for each interval. See Johnson and others (2011) for original data. %TOC calculated from Fischer Assay gallons per ton via the simplified formula %TOC = 0.4*GPT + 1 (see Figure 6).

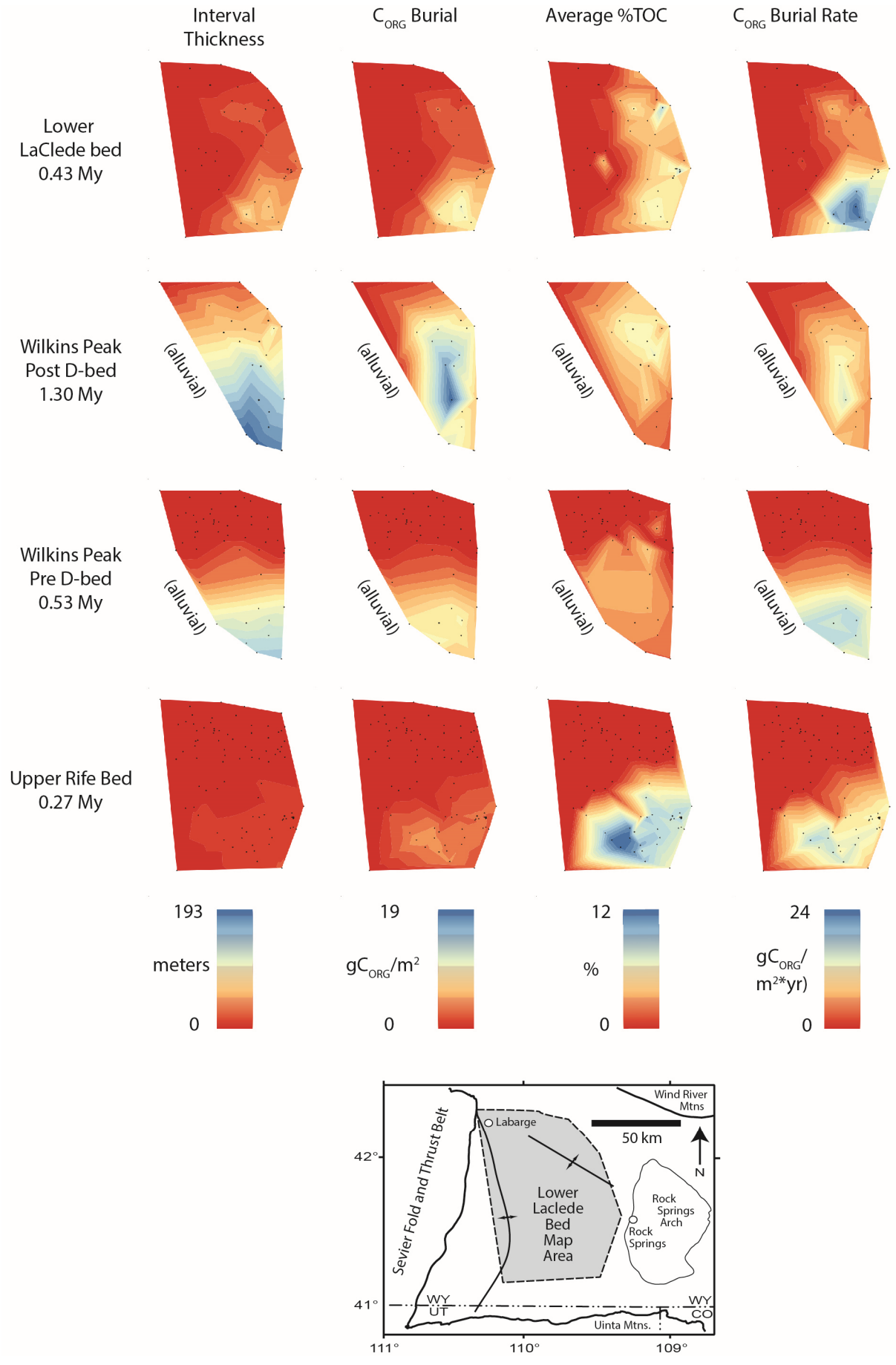


Figure 8. Patterns of net accumulation, relative organic matter enrichment and net accumulation rates for four study intervals in the Bridger basin. Map area varies for each interval depending on the lateral limits of organic -rich beds.

is the southward thickening of the Wilkins Peak Member. The most pronounced thickness gradient occurring in the its lower part, whereas the upper part is generally thicker overall. The other two units show more subtle thickening to the southeast. These patterns indicate generally greater accommodation rates in the southern Bridger Basin. C_{ORG} burial reaches a maximum in the southeast map area for the upper Rife Bed, lower Wilkins Peak Member, and lower La-Clede Bed, but the maximum rates coincide with the eastern map area for the upper Wilkins Peak Member. The highest average %TOC occurs in the southeast mapped area of the upper Rife bed. The highest values in the lower Wilkins Peak Member are displaced northward relative to its maxima in thickness and C_{ORG} burial, indicating the former decreases northward more rapidly than the latter. The upper Wilkins Peak Member maximum %TOC shifts to the northeast mapped area, and the lower LaClede maximum values are distributed across the eastern mapped area.

The C_{ORG} burial rate column brings in the added dimension of time, and reveals a pattern of higher values in the south or southeastern mapped areas for three of the four mapped intervals. The upper Wilkins Peak Member shows a different pattern, with maximum values shifted farther north. Integration of the contour maps allows calculation of average C_{ORG} burial fluxxes (Table 3), which are notably consistent at 4–5 g/m²yr for all four time intervals. The tuff ages used to estimate the duration of each interval typically

have 2σ error ranges of ± 100 ky, and further errors may have been introduced by interpolation between ages or in the mapping process. Based on the stratigraphic positions of dated tuffs, their age uncertainties, and the interval durations, the upper Wilkins Peak Member C_{org} burial rates are likely the most reliable and the upper Rife Bed C_{org} burial rates the least. However, even if the calculated average rates are off by 2x they would still be nearly an order of magnitude less than the average Minnesota lakes rate reported by Dean and Gorham (1998; Table 3).

Inorganic Carbon Burial

Carbonate minerals (principally calcite and dolomite with lesser Na-carbonate) contribute a large additional component of carbon burial in the Green River Formation. This component is not measured by Fischer assay; the estimates presented here are therefore based on total interval thickness and subject to uncertainties related to differences between actual mineralogy versus the simplifying assumption of constant mineralogy (50% carbonate versus other minerals). Despite this limitation these estimates are useful for gross comparison of organic and inorganic carbon (C_{INORG}) burial.

To a first approximation, organic and (C_{INORG}) burial rates were subequal (Table 4). The lowest calculated (C_{INORG}) burial rate occurred during deposi-

Table 3	Organic	Carbon	Ruvial in	Ancient	and Mode	wn Lakes
ranie 5.	Organic	Carbon	Duriai in	Ancieni	ana moae	rn Lakes

Unit	Area (10 ⁹ m ²)	C _{ORG} burial rate (10 ⁹ gC/yr)	C _{ORG} burial flux (gC/m²yr)
Bridger Basin:			
Lower Laclede Bed	8.2	43	5
Wilkins Peak Member (post-D)	8.4	36	4
Wilkins Peak Member (pre-D)	6.3	31	5
Upper Rife Bed	8.9	35	4
*Hypothetical maximum	10.0	440	44
**Junggar-Turpan-Hami basin (China)	300	3900	13
***Qinghai Lake (China)	30	180	6
***Lake Turkana (east Africa)	123	1353	11
*****Minnesota lakes	14	1,000	72
***Small northern hemisphere lakes	320	23,000	72
****All lakes and inland seas	2500	42,000	5

^{*}Assumes an interval 0.5 m thick with 20% TOC, deposited over 5000 years at a rate of 100x10⁻⁶ m/yr.

^{**}Permian (Carroll and Wartes, 2003)

^{**}Einsele and others (2001)

^{***}Dean and Gorham (1998).

Table 4. Inorganic Carbon Burial Rates.

	C _{INORG} burial rate	C _{INORG} burial flux
Unit	(10^9g/yr)	(g/m^2yr)
Lower Laclede Bed	61	7
Wilkins Peak Member (post-D)	48	6
Wilkins Peak Member (pre-D)	71	11
Upper Rife Bed	32	4

tion of the upper Rife Bed, as expected based on its relatively high %TOC. The calculated $C_{\rm INORG}$ rate is likely an overestimate, due to the fact that this interval has a higher clay content than succeeding intervals (Mason, 2012). The other intervals have calculated rates of $C_{\rm INORG}$ burial that are slightly greater than $C_{\rm ORG}$ burial rates, but the apparent differences may not be significant.

DISCUSSION

Lake Basin Morphology and Organic Matter Distribution

The strikingly dissimilar frequency distributions of Fischer assay GPT for fluctuating-profundal versus evaporative facies associations (Figure 7) attest to important first-order differences in how organic matter was preserved within each. Previous studies have concluded that organic matter in these facies associations is dominantly autochthonous, produced by cyanobacteria and algae within the lake (e.g. Bradley, 1929; Horsfield and others, 1994; Carroll and Bohacs, 2001). It therefore is unlikely that the different enrichment patterns observed in this study reflect different admixtures of aquatic versus terrestrial organic matter types. Differences in the balance of primary productivity versus organic matter preservation also seem an unlikely explanation since average net rates of organic matter burial were essentially the same for all four study intervals (Table 3).

We propose that differences in GPT histograms reflect the bimodal hypsometry of the basin that Lake Gosiute occupied. The late Quaternary history of the Lake Bonneville basin in Utah offers a useful analog (site of Great Salt Lake). The floor of the Bonneville basin is relatively flat, with shallow gradients generally ≤1 m per km. In contrast, the topography of the Wasatch Mountains that bound the basin to the east is much steeper, on the order of 100's of m per km. Modern Great Salt Lake has fluctuated over range of ∼6 m in depth over historical timescales, but even during its maxima it has been confined to the low-

gradient basin floor. Small changes in depth therefore result in large changes in surface area. Earlier lake stages in the Bonneville basin rose as high as ~300 m above the present lake surface however, forming the well-known shoreline features on the slopes of Wasatch Mountains and other ranges (Gilbert, 1890). At those high levels changes in lake depth resulted in relatively small changes in lake surface area.

The lateral limits of the Wilkins Peak Member are typically defined by gradual transitions into alluvial facies (Smoot, 1983; Roehler, 1992; Pietras and Carroll, 2006; Smith and others, 2015), consistent with confinement of Lake Gosiute to a relatively lowgradient basin floor (Figure 9). High-frequency (e.g., Milankovitch band) fluctuations in lake depth would thus have caused large changes in lake area. Carroll and Bohacs (2001) showed that organic matter enrichment of the Wilkins Peak Member correlates with facies evidence for increased lake depth. Organic-rich deposits thus correspond to highstands, but these events were relatively rare due to the hydrologic limitations of a generally dry basin (cf. Bohacs and others, 2000). The volume of water needed to fill the lake would have increased in proportion to the square of its depth, as would evaporation. Spring deposits occur commonly near the basin margins (e.g., Leggit and Cushman, 2001; Awramik and Buchheim, 2017), and groundwater discharge may have contributed significantly to the lake's hydrologic budget (Baddouh and others, 2020; Jagniecki and others, 2021). During most of Wilkins Peak Member deposition some portion of the lake floor was exposed and subject to organic matter oxidation, as evidenced by the abundant occurrence of mudcracks (Smoot, 1983; Pietras and Carroll, 2006), resulting in the observed predominance of low GPT measurements.

In contrast, the upper Rife and lower LaClede Beds are interpreted to record deposition when the lake intersected the basin-bounding uplifts. The basin floor remained mostly submerged except during short -lived lowstands. Evidence for lake desiccation is rare in the upper Rife Bed (Graf and others, 2015); very few samples yield less than 3 GPT. The lower LaClede Bed does display evidence for repeated desic-

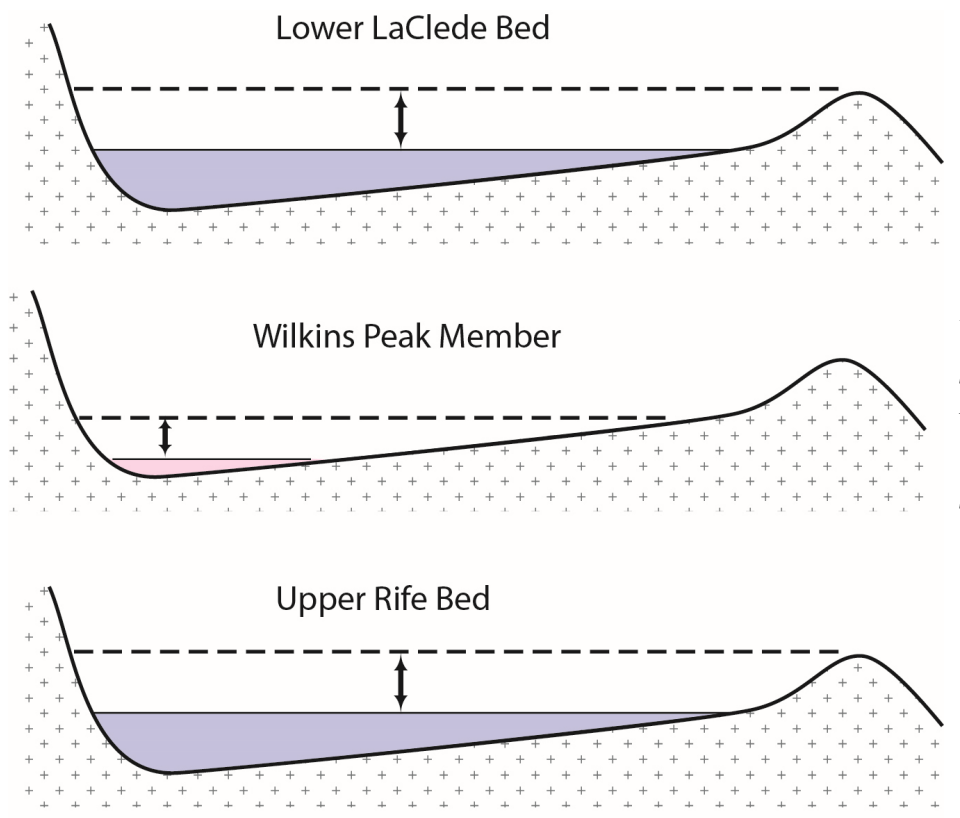


Figure 9. Schematic illustration of basin hypsometry and lake levels associated with underfilled (Wilkins Peak Member) versus balanced-fill (upper Rife and lower LaClede Beds) basin phases. Vertical arrow represents inferred range of high-frequency lake level changes.

cation (Surdam and Stanley, 1979; Rhodes and Carroll, 2015), consistent with the more plentiful occurrence of low GPT measurements. Both fluctuating-profundal units record more continuous deposition of organic-rich strata than the evaporative Wilkins Peak Member however.

Intrabasinal Patterns of Organic Matter Burial

Basin-scale C_{ORG} burial rates are similar for all four intervals included in this study, but the geographic patterns of organic matter enrichment exhibit two distinct modes, corresponding to fluctuating profundal versus evaporative facies associations. The former is characterized by relatively uniform interval thickness across the mapped area, particularly in the case of the upper Rife Bed (Figures 3, 8). Based on tuff ages Smith and others (2008) estimated relatively slow accumulation rates for the fluctuating profundal intervals, on the order of 100 μ m/yr. Slow burial of organic matter may imply that a salinity-stratified water column helped to maintain low-oxygen bottom waters that enhanced preservation (c.f. Carroll and Bohaes, 2001).

Despite their relatively uniform thickness patterns, the upper Rife and lower LaClede beds, C_{ORG} burial and burial rates in these intervals is strongly focused on the southeast corner of the mapped area.

This pattern may indicate that the lake was deeper there, and therefore the lake floor was more likely to remain below the chemocline. Alternatively, local influx of nutrients carried by streams may have resulted in increased productivity and an enhanced oxygen minimum zone. Based on sandstone paleocurrents and detrital zircon ages, Hammond and others (2019) argued that the Aspen paleoriver entered the southeast Bridger Basin during Wilkins Peak Member deposition, supplying excess bicarbonate needed to precipitate Na-carbonate evaporite. It may also have carried nutrients such as phosphorous, sulfur, magnesium, and calcium, derived from Paleozoic and Mesozoic strata within its watershed (Bohacs and others, 2007)

The evaporative Wilkins Peak Member contains a smaller overall proportion of C_{ORG} but was deposited $\sim 3x$ faster than the fluctuating profundal intervals above and below (Smith et at., 2008). The southward thickening of the lower Wilkins Peak has been previously attributed to tectonic accommodation related to frontal faulting of the Uinta uplift (Roehler, 1992; Pietras and Carroll, 2006; Smith and others, 2015). Downward flexure of the adjacent lithosphere likely resulted in a foredeep near the Uinta uplift during lake highstands, where salinity stratification may have occurred. Rapid accumulation of inorganic sediment diluted organic matter, but may also have enhanced its preservation by limiting the time during which it was exposed to atmospheric oxygen. The highest C_{ORG} burial rates thus correspond to the

southern mapped area, where organic matter productivity may also have been enhanced by the Aspen paleoriver. The pronounced northward shift in C_{ORG} burial in the upper Wilkins Peak Member coincides with a northward shift in the locus of bedded evaporite preservation and reduction in its volume (Wiig, 1995). Both changes are interpreted to have resulted from a cessation of range-front faulting (Roehler, 1992).

Role of Eocene Lakes in the Global Carbon Cycle

Green River Formation lakes clearly buried a large amount of C_{ORG}. The Bridger basin units in this study are estimated to contain ~92 Gt C_{ORG}, which does not include C_{ORG} in freshwater lacustrine deposits or lacustrine strata in adjacent basins in Colorado and Utah. Johnson et al (2001) estimated that the total oil generative potential of all these deposits together totals ~4.3 trillion barrels, equivalent to ~490 Gt of C_{ORG}. Green River Formation spanned 8–9 My however, raising the question of whether annual burial rates were large enough to influence global climate. Dividing 490 Gt by 8 My gives an average annual C_{ORG} burial rate of 6.1 x 10^{10} g/yr. For comparison, Dean and Gorham (1998) estimated that Holocene freshwater lakes in the northern hemisphere bury ~4.2 x 10^{13} g/yr, equal to 42% of the total C_{ORG} burial rate of the ocean.

The results of this study indicate that average Eocene C_{ORG} burial fluxes in the Bridger Basin are roughly comparable to those reported for other large, saline or hypersaline lakes (Table 3). The Permian Junggar-Turpan-Hami basin in northwest China has calculated gC/m²yr values approximately three times higher than the Bridger basin, but it must be noted that these saline to hypersaline lake deposits lack reliable radioisotopic dating. C_{ORG} fluxes are therefore based on the assumption that laminations in organic-facies are annual in origin (Carroll and Wartes, 2003). Hypersaline Qinghai Lake and saline Lake Turkana have estimated C_{ORG} are similar to those Bridger basin (Einsele et al., 2001), although these estimates apparently depend on extrapolation of limited facies observations and therefore may embody large uncertainties.

Based on the simplifying assumption that Green River Formation marlstone contains an average of 50% carbonate minerals, burial rates of $C_{\rm INORG}$ were similar in magnitude to $C_{\rm ORG}$ (Table 4), although this estimate is subject to large uncertainties. Some of the $C_{\rm INORG}$ likely derived from dissolution of Paleozoic and Mesozoic marine limestone, which presently are exposed adjacent to the Bridger Basin in the northern

flank of the Uinta Mountains and in the Sevier fold and thrust belt. This contribution would not be expected to make a net impact on the global carbon cycle however, because it was simply transferred from one geologic reservoir to another. Additional C_{INORG} must also have derived from silicate weathering, based on ⁸⁷Sr/⁸⁶Sr ratios in Green River Formation marlstone. In the Bridger Basin these fall in the range of $\sim 0.711-0.715$ (Rhodes and others, 2002; Doebbert and others, 2014; Baddouh and others, 2016, 2017). In contrast, primary marine carbonate ratios that are generally <0.7095 (e.g., Veizer and others, 1999). The more radiogenic ⁸⁷Sr/⁸⁶Sr ratios in the Green River Formation therefore require hydrolysis of silicate rocks, in which ⁸⁷Sr/⁸⁶Sr is commonly >0.720, in addition to dissolution of marine carbonate. The importance of silicate weathering in C_{INORG} burial depends on the relative concentrations of Sr in silicate rocks versus marine carbonate, both of which are variable.

Although the average carbon burial rates in the Bridger Basin were lower than those in late Holocene Minnesota lakes, such direct comparison is problematic for several reasons. The Green River Formation strata considered in this study were deposited in large saline to hypersaline lakes that accumulated dominantly aquatic organic matter (Carroll and Bohacs, 2001), whereas the northern hemisphere Holocene lakes described by Dean and Gorham (1998) are generally smaller and freshwater. Advection of terrestrial organic matter latter may account for a substantial fraction of the organic matter deposited in the postglacial freshwater lakes, and higher sedimentation rates may have aided in its preservation. In contrast, organic matter preservation in more slowly-deposited saline lakes typically relies on the establishment of stable salinity stratification. Another important difference lies in the grossly dissimilar timescales represented by ancient lake deposits versus Holocene lake sediment. The former records organic matter burial (and diagenesis) averaged over $\sim 10^5$ yr or greater timescales, compared to which Holocene sedimentation is a virtual "snapshot" in Earth history. Sadler (1981) noted that calculated accumulation rates generally tend to vary inversely with the interval duration, due to the greater probability of incorporating hiatuses. This effect may be less important in a closed basin, but the possibility of unrecognized hiatuses cannot be entirely excluded for the Bridger Basin.

An alternative approach would be to compare rates of C_{ORG} burial by small Holocene lakes to the maximum rates of burial in the Bridger Basin. Holocene C_{ORG} burial is largely attributable to lake basins created in the wake of retreating ice sheets, a geologically transient event. A valid comparison to the Bridger Basin should therefore be based on a similar-

ly transient Eocene event—specifically, the deposition of a single organic rich bed. Organic matter content in the Bridger Basin commonly varies over a range of 0–20% TOC over thickness scales of a few meters (Horsfield and others, 1994; Carroll and Bohacs, 2001; Figures 3, 4), and the most organic-rich beds have been tied to precessional-scale climate forcing (Meyers, 2008; Machlus and others, 2008). Maximum rates of C_{ORG} burial in the Bridger Basin can be estimated based on the average accumulation rate of fluctuating profundal facies, which consist largely of laminated organic-rich marlstone, or by assuming that laminae are annual in origin. The first method yields rates on the order of 100 µm/yr (Smith and others, 2008), and the laminae are commonly ~100 µm thick. Although not proof, this correspondence is at least permissive of an annual origin of laminae. Based on a hypothetical bed 0.5 m thick with 20% TOC that accumulated over a time interval of 5000 years (equivalent to the late Holocene), the maximum rate of C_{ORG} burial in the Bridger basin was an order of magnitude higher than the average rate, and broadly equivalent to estimated average global rates for Holocene lakes (Table 3).

In order to represent a globally significant carbon flux, lakes also need to cover a relatively large surface area across which high C_{ORG} burial rates occurred synchronously. The areal extent of Holocene lakes is readily measurable, and their synchronicity is easy to test. Unfortunately, neither is true for Eocene lakes. Together, the maximum area covered by Lake Gosiute and coeval Lake Uinta (located to the south of Lake Gosiute) was $\sim 3x$ the mapped area in this study (Johnson and others, 2011). Eocene lake deposits have been reported in other areas as well (e.g., Carroll and others, 2010), but their total extent is unknown. In order to play a significant role in the global carbon cycle their burial histories would likely need to be closely synchronized, perhaps via astronomical forcing, but at present their relative timing is poorly known.

Returning at last to the question of whether carbon burial in the Green River Formation contributed to the demise of the EECO (cf. Hood and Cole, 2015), it is noteworthy that these two events partly coincided in time (Smith et al., 2003). The EECO spanned ~53–50 Ma (Zachos and others, 2008), compared to ~51.8–49.2 Ma for the units examined in this study (Table 1). The timing of the stratigraphically lowest, freshwater Green River Formation strata is less well constrained due to an absence of tuff beds predating the Tipton Member, but the onset of lacustrine sedimentation has been projected to have occurred at ~53 Ma (Smith and others, 2008). It thus appears that rather than heralding the end of the

EECO, initial carbon burial in the Green River Formation approximately coincided with the EECO onset. The carbon burial rates reported in this study appear essentially invariant though time during the EECO (Table 1). Green River Formation deposition continued during the period of decreasing oceanbottom temperature that followed the EECO (Zachos and others, 2008), but the total area of Eocene lakes progressively decreased through ~44 Ma (Smith and others, 2008). These observations do not appear to directly support the hypothesis that massive lacustrine carbon burial caused post-EECO cooling (cf. Hood and Cole, 2015). The episodic recurrence of fluvial siliciclastic facies in the Wilkins Peak Member does suggest that major fluctuations in carbon burial occurred at ~100 ky intervals however, paced by short eccentricity (Aswasereelert and others, 2013). Smith and others (2014) proposed that the fluvial facies correspond to hyperthermal events, that correspond to sharp declines in carbon burial. Further research is required to ascertain the relationship of these fluctuations to Eocene hyperthermals identified in marine records (e.g., Lauretano and others, 20216), and to changes in $[CO_2]_{atm}$.

CONCLUSIONS

Fischer assay analyses of the lacustrine Green River Formation offer a rare opportunity to quantitatively assess spatial patterns of organic matter accummulation at the basin scale. Coupled with recent advances in the radioisotopic geochronology of intercalated volcanic tuff beds, Fischer assay data also provide a means of directly measuring burial rates of sedimentary organic matter and their relationship to sedimentary facies associations.

Two distinctly different patterns of organic matter enrichment characterize evaporative versus fluctuating profundal facies associations. The evaporative facies association exhibits an approximately exponential decline in Fischer assay gallons of oil per ton (GPT) versus frequency, with a mode of 0-1 GPT. This pattern is interpreted to reflect episodic oscillation of a hypersaline lake across a low-gradient underfilled basin floor, that experienced frequent desiccation. The highest rates of organic matter burial generally coincided with areas of more rapid basin accommodation. In contrast, the fluctuating profundal facies association exhibits an approximately normal or log normal distribution of GPT, with modal values as high as 16–18. This pattern is interpreted to reflect generally deeper conditions when the lake surface intersected the bounding uplifts of a balanced-fill basin. Organic matter burial rates were more uniformly distributed across the Bridger basin.

The net flux of organic matter into Bridger basin strata was essentially invariant across the temporal window examined in this study. Dilution by inorganic sediment appears to have exerted a primary control on preserved organic matter enrichment.

Previous estimates of organic matter burial by Holocene freshwater lakes in the northern hemisphere have led to the inference that such lakes constitute a significant element of the global carbon cycle. Organic matter burial fluxes (gC/m²) measured in this study for saline to hypersaline lakes are an order of magnitude lower than for Holocene freshwater lakes however. This difference may in part reflect differences in sedimentary facies or lake chemistry. Inorganic carbon in carbonate minerals also contributes substantially to total Green River Formation carbon burial, although inorganic carbon burial rates are not well constrained. More fundamentally, postglacial Holocene lakes represent geologically ephemeral, synchronized deposition across a large part of the northern continents. In contrast, Green River Formation rates are time-averaged over intervals of 10⁵– 10⁶ yrs. Maximum burial fluxes over shorter time frames ($\sim 10^3$ yrs) were likely much higher. The detailed temporal relationship of the Green River Formation to other Eocene lake deposits is largely unknown, but global lacustrine carbon burial synchronized via Milankovic-scale climatic forcing could enhance their potential climatic impact. However, the timing of Green River Formation organic matter burial appears inconsistent with a previous proposal that it brought about the end of the Early Eocene Climatic Optimum.

ACKNOWLEDGEMENTS

Funding for this study was provided by the Rocky Mountain Association of Geologists, the Society for Sedimentary Geology (SEPM), the Jay Nania Foundation, the Center for Oil Shale Technology and Research (COSTAR), the University of Wisconsin-Madison Department of Geoscience, and NSF-IES 1813278. The authors are grateful to J. Czaplewski, and M. McClennen, R. Johnson, and M.E. Smith for their assistance or discussions, and to J.T Pietras and an anonymous reviewer or their thoughtful comments on the manuscript.

REFERENCES CITED

Archer, D, 2005, Fate of fossil fuel CO₂ in geologic time: Journanl of Geophysical Research, v. 110, C09S05, doi:10.1029/2004JC002625

Aswasereelert, W., Meyers, S.R., Carroll, A.R., Pe-

- ters, S.E., Smith, M.E., and Feigl, K.L., 2013, Basin-scale cyclostratigraphy of the Green River Formation, Wyoming: Geological Society of America Bulletin, v. 125, p. 216–228, doi: 10.1130/B30541.1.
- Awramik, S.M. and Buchheim, H.P., 2016, Giant stromatolites of the Eocene Green River Formation (Colorado, USA): Geology, v. 43, 691–694
- Baddouh, M., Carroll, A.R., Meyers, S.R., Beard, B.L., and Johnson, C.M., 2017, Chronostratigraphic correlation of lacustrine deposits using 87Sr/86Sr ratios, Eocene Green River Formation, Wyoming: Journal of Sedimentary Research, v. 87, p. 406-423.
- Baddouh, M., Jagniecki, E.A., Carroll, A.R., Beard, B.L., Lowenstein, T.K., and Johnson, C.M., 2020, Groundwater Mixing in an Alkaline Paleolake: Eocene Green River Formation, Wyoming: Palaeogeography, Palaeoclimatology, Palaeoecology v. 561, 110038.
- Baddouh, M., Meyers, S.R., Carroll, A.R., Beard, B.L., and Johnson, C.M., 2016, Lacustrine ⁸⁷Sr/⁸⁶Sr as a tracer to reconstruct 1 Milankovitch forcing of the Eocene hydrologic cycle: Earth and Planetary Science Letters, v. 448, p. 62-68.
- Bohacs, K., Carroll, A., Nede, J.E., and Mankirowicz, P.J., 2000, Lake-Basin Type, Source Potential, and Hydrocarbon Character: An Integrated Sequence-Stratigraphic-Geochemical Framework, *in* (E. H. Gierlowski-Kordesch and K. R. Kelts, Eds): Lake basins through space and time: AAPG Studies in Geology #46, p. 3–34.
- Bohacs, K.M., Grabowski, G., and Carroll, A.R., 2007, Lithofacies architecture and variations in expression of sequence stratigraphy within representative intervals of the Green River Formation, Greater Green River Basin, Wyoming and Colorado: Rocky Mountain Association of Geologists, v. 44, p. 39-60.
- Bohacs, K.M., Grabowski, G.J., Carroll, A.R., Mankiewicz, P.J., Miskell-Gerhardt, K.J., Schwalbach, J.R., Wegner, M.B., and Simo, J.A., 2005, Production, destruction, and dilution; the many paths to source-rock development (N. B. Harris, Ed.): The Deposition of Organic-Carbon-Rich Sediments: Models, Mechanisms, and Consequences. Special Publication Society for Sedimentary Geology, v. 82, p. 61–101.
- Bradley, W.H., 1929, The varves and climate of the Green River epoch: U.S. Geological Survey Professional Paper 158-E, 110 p.
- Bradley, W.H., 1964, Geology of Green River Formation and associated Eocene rocks in southwestern Wyoming and adjacent parts of Colorado and

- Utah: Professional Paper USGS Numbered Series 496–A, http://pubs.er.usgs.gov/publication/ pp496 A (accessed July 2016).
- Carroll, A.R., 2017, Xenoconformities and the stratigraphic record of paleoenvironmental change: Geology, v. 45, p. 639-642.
- Carroll, A.R., and Bohacs, K.M., 1999, Stratigraphic classification of ancient lakes: Balancing tectonic and climatic controls: Geology, v. 27, p. 99–102, doi: 10.1130/0091-7613(1999)027<0099:SCOA-LB>2.3.CO;2.
- Carroll, A.R., and Bohacs, K.M., 2001, Lake-type controls on petroleum source rock potential in nonmarine basins: AAPG Bulletin, v. 85, p. 1033 –1053.
- Carroll, A.R., Graham, S.A., and Smith, M.E., 2010, Walled sedimentary basins of China: Basin Research, v. 22, p. 17-32.
- Carroll, A. R., and Wartes, M. A., 2003, Organic Carbon Burial by Large Permian Lakes, Northwest China, *in* Chan, M. A., and Archer, A. W., eds., Extreme depositional environments: mega end members in geologic time: Geological Society of America Special Paper 370, p. 91-104.
- Cole, J.J., Prairie, Y.T., Caraco, N.F., McDowell, W.H., Tranvik, L J., Striegl, R.G., Duarte, C.M., Kortelainen, P., Downing, J.A., Middelburg, J.J., and Melack, J., 2007, Plumbing the global carbon cycle: Integrating inland waters into the terrestrial carbon budget: Ecosystems, v. 10, p. 171–184.
- Cook, E.W., 1974, Green River shale-oil yields: correlation with elemental analysis: Fuel, v. 53, p. 16 –20, doi: 10.1016/0016-2361(74)90026-X.
- Culbertson, W.C., 1961, Stratigraphy of the Wilkins Peak Member of the Green River Formation, Firehole Basin Quadrangle, Wyoming: U.S. Geological Society, Professional Paper 424D, p. 170–173.
- Dean, W.E., and Gorham, E., 1998, Magnitude and significance of carbon burial in lakes, reservoirs, and peatlands: Geology, v. 26, p. 535–538, doi: 10.1130/0091-7613(1998) 026<0535:MASOCB>2.3.CO;2.
- Dean, W.E., and Gorham, E., 19989, Magnitude and significance of carbon burial in lakes, reservoirs, and peatlands: Geology, v. 26, p. 535-538.
- Dickinson, W.R., Klute, M.A., Hayes, M.J., Janecke, S.U., Lundin, E.R., McKittrick, M.A., and Olivares, M.D., 1988, Paleogeographic and paleotectonic setting of Laramide sedimentary basins in the central Rocky Mountain region: Geological Society of America Bulletin, v. 100, p. 1023–1039, doi: 10.1130/0016-7606(1988)100<1023-:PAPSOL>2.3.CO;2.
- Doebbert, A.C., Carroll, A.R., Mulch, A., Chetel, L.M., and Chamberlain, C.P., 2010, Geomorphic

- controls on lacustrine isotopic compositions; evidence from the Laney Member, Green River Formation, Wyoming: Geological Society of America Bulletin, v. 122, p. 236–252, doi: http://dx.doi.org.ezproxy.library.wisc.edu/10.1130/B26522.1.
- Doebbert, A.C., Johnson, C.M., Carroll, A.R., Beard, B.L., Pietras, J.T., Rhodes Carson, M., Norsted, B., and Throckmorton, L.A., 2014, Controls on Sr isotopic evolution in lacustrine systems: Eocene Green River Formation, Wyoming: Chemical Geology, v. 380, p. 172-189.
- Downing, J.A., and 10 others, 2006, The Global Abundance and Size Distribution of Lakes, Ponds, and Impoundments: Limnology and Oceanography, v. 51, p. 2388–2397.
- Duarte, C.M., Prairie, Y.T., Montes, C., Cole, J.J., Striegl, J.M., Melack, J., and Downing, J.A., 2008, CO₂ emissions from saline lakes: A global estimate of a surprisingly large flux: Journal of Geophysical Research, VOL. 113, G04041, doi:10.1029/2007JG00063.
- Einsele, G., Yan, J., and Hinderer, M., 2001, Atmospheric carbon burial in modern lake basins and its significance for the global carbon budget: Global and Planetary Change, v. 30, p. 167-195.
- Fischer, F., and Schrader, H., 1920, Urteerbestimmungen mit einem Aluminium-schwelapparat: Angewandte Chemie, v. 33, p. 172–175, doi: 10.1002/ange.19200335607.
- Gilbert, G.K., 1890, Lake Bonneville: Geological Survey Monograph 1, 438 p.
- Goodfellow, L., and Atwood, M.T., 1974, Fischer assay of oil shale; procedures of the Oil Shale Corporation: Quarterly of the Colorado School of Mines, 1906-, v. 69, p. 205–219.
- Graf, J.W., Carroll, A.R., and Smith, M.E., 2015, Lacustrine Sedimentology, Stratigraphy and Stable Isotope Geochemistry of the Tipton Member of the Green River Formation, *in* (Smith, M.E. and Carroll, A.R. Eds.): Stratigraphy and Paleolimnology of the Green River Formation, Western USA, Syntheses in Limnogeology 1, p. 31–60.
- Graf, J.W., Carroll, A.R., and Smith, M.E., 2015, Lacustrine sedimentology, stratigraphy and stable isotope geochemistry of the Tipton Member of the Green River Formation, *in* Smith, M.E., and Carroll, A.R. (eds.), Stratigraphy and Paleolimnology of the Eocene Green River Formation, Western U.S.: Springer, p. 31-60.
- Hammond, A.P., Carroll, A.R., Smith, M.E., and Lowenstein, T.K., 2019, The Aspen Paleoriver: Linking Eocene Magmatism to the World's Largest Na-Carbonate Evaporite: Geology, v. 47, p. 1020-1024.

- Heistand, R.N., 1976, Fischer assay, a Standard Method?, American Chemical Society, Division of Fuel Papers, v. 21, p. 40-54
- Heistand, R.N., and Humphries, H.B., 1976, Direct determination of organic carbon in oil shale: Analytical Chemistry, v. 48, p. 1192–1194, doi: 10.1021/ac50002a032...
- Hood W.C., and Cole, R.D., 2015, Did the Eocene Green River Lakes Change Earth's Climate?, *in* (Rosen, M.R., Cohen, A., Kirby, M., Gierlowski-Kordesch, E., Starratt, S., Valero Garcés, B.L., and Varekamp, J., eds.): Sixth International Limnogeology Congress—Abstract Volume, Reno, Nevada, June 15–19, 2015: U.S. Geological Survey Open-File Report 2015-1092, p. 93, http://dx.doi.org/10.3133/ofr20151092.
- Horsfield, B., Curry, D.J., Bohacs, K., Littke, R., Rullkoetter, J., Schenk, H.J., Radke, M., Schafer, R.G., Carroll, A.R., Isaksen, G., and Witte, E.G., 1994, Organic geochemistry of freshwater and alkaline lacustrine sediments in the Green River Formation of the Washakie Basin, Wyoming, U.S.A. (N. Telnaes, Ed.): Organic Geochemistry, v. 22, p. 415–440.
- Jagniecki, E.A., Lowenstein, T.K., Demicco, R.V., Baddouh, M., Carroll, A.R, Beard, B.L., Johnson, C.M., 2021, Spring Origin of Eocene Carbonate Mounds in the Green River Formation, northern Bridger Basin, Wyoming: Sedimentology, v. 68, p.?.doi: 10.1111/sed.12852.
- Jagniecki, E.A., and Lowenstein, T.K., 2015, Evaporites of the Green River Formation, Bridger and Piceance Creek Basins: Deposition, Diagenesis, Paleobrine Chemistry, and Eocene Atmospheric CO2, , *in* Smith, M.E., and Carroll, A.R. (eds.), Stratigraphy and Paleolimnology of the Eocene Green River Formation, Western U.S.: Springer, p. 277-312.
- Johnson, R.C., Mercier, T.J., Ryder, R.T., Brownfield, M.E., and Self, J.G., 2011, Assessment of in -place oil shale resources of the Eocene Green River Formation, Greater Green River Basin, Wyoming, Colorado, and Utah, *in* U.S. Geological Survey Oil Shale Assessment Team, ed., Oil shale resources of the Eocene Green River Formation, Greater Green River Basin, Wyoming, Colorado, and Utah: U.S. Geological Survey Digital Data Series DDS-69-DD, chap. 1, 63 p., 1 plate.
- Keighin, C.W., 1980, Comparison of Fischer assay data generated by four laboratories: The Mountain Geologist, v. 17, No. 1, p. 13-21.
- Lauretano, V., Hilgen, F.J., Zachos, J.C., and Lourens, L.J. (2016), Astronomically tuned age model for the early Eocene carbon isotope events: A new high-resolution δ13C benthic record of

- ODP Site 1263 between \sim 49 and \sim 54 Ma: Newsletters on Stratigraphy, 4v. 9, p. 83–400, doi: 10.1127/nos/2016/0077.
- Leggitt, V.L. and Cushman Jr, R.A., 2001, Complex caddisfly dominated bioherms from the Eocene Green River Formation: Sedimentary Geology, v. 145, p. 377–396.
- Love, J.D., 1960, Cenozoic sedimentation and crustal movement in Wyoming: American Journal of Science, v. 258-A, p. 204–214.
- Machlus, M.L., Olsen, P.E., Christie-Blick, N., and Hemming, S.R., 2008, Spectral analysis of the lower Eocene Wilkins Peak Member, Green River Formation, Wyoming: Support for Milankovitch cyclicity: Earth and Planetary Science Letters, v. 268, p. 64–75, doi: 10.1016/j.epsl.2007.12.024.
- Machlus, M.L., Ramezani, J., Bowring, S.A., Hemming, S.R., Tsukui, K., and Clyde, W.C., 2015, A strategy for cross-calibrating U–Pb chronology and astrochronology of sedimentary sequences: An example from the Green River Formation, Wyoming, USA: Earth and Planetary Science Letters, v. 413, p. 70–78, doi: 10.1016/j.epsl.2014.12.009.
- Macquaker, J.H.S., and Howell, J.K., 1999, Small-scale (<5.0 m) vertical heterogeneity in mudstones: implications for high-resolution stratigraphy in siliciclastic mudstone successions: Geological Society of London, Journal, v. 156, p. 105–112.
- Mason, G.M., 2012, Stratigraphic distribution and mineralogic correlation of the Green River Formation, Green River and Washakie Basins, Wyoming, U.S.A. In Baganz, O.W., Bartov, Y., Bohacs, K., Nummedal, D. (Eds.), Lacustrine Sandstone Reservoirs and Hydrocarbon Systems: AAPG Memoir, v. 95. p. 223–253.
- Meyers, S.R., 2008, Resolving Milankovitchian controversies: The Triassic Latemar Limestone and the Eocene Green River Formation: Geology, v. 36, p. 319–322, doi: 10.1130/G24423A.1.
- Middleton, G.V., 1973, Johannes Walther's Law of the Correlation of Facies: Geological Society of America Bulletin, v. 84, p. 979-988.
- Passey, Q.R., Bohacs, K.M., Esch, W.L., Klimentidis, R., and Sinha, S., 2010, From Oil-Prone Source Rock to Gas-Producing Shale Reservoir: Geologic and Petrophysical Characterization of Unconventional Shale-Gas Reservoirs: Society of Petroleum Engineers, no. 131350, 29 p.
- Pietras, J.T., and Carroll, A.R., 2006, High-resolution stratigraphy of an underfilled lake basin; Wilkins Peak Member, Eocene Green River Formation, Wyoming, U.S.A.: Journal of Sedimentary Research, v. 76, p. 1197–1214, doi: http://

- dx.doi.org.ezproxy.library.wisc.edu/10.2110/jsr.2006.096.
- Pietras, J.T., Carroll, A.R., and Rhodes, M.K., 2003a, Lake basin response to tectonic drainage diversion: Eocene Green River Formation, Wyoming: Journal of Paleolimnology, v. 30, p. 115–125, doi: 10.1023/A:1025518015341.
- QGIS Development Team, 2014, QGIS Geographic Information System, Open Source Geospatial Foundation Project, http://www.qgis.org/
- Rhodes Carson, M.K., and Carroll, A.R., 2015, Lake Type Transition from Balanced-Fill to Overfilled: Laney Member, Green River Formation, Washakie Basin, Wyoming, *in* Smith, M.E., and Carroll, A.R. (eds.), Stratigraphy and Paleolimnology of the Eocene Green River Formation, Western U.S.: Springer, p. 103-125.
- Rhodes, M.K., Carroll, A.R., Pietras, J.T., Beard, B.L., and Johnson, C.M., 2002, Strontium isotope record of paleohydrology and continental weathering, Eocene Green River Formation, Wyoming: Geology, v. 30, p. 167–170, doi: 10.1130/0091-7613(2002)030<0167:SIROPA>2.0.CO;2.
- Roehler, H.W., 1992, Correlation, composition, areal distribution, and thickness of Eocene stratigraphic units, greater Green River basin, Wyoming, Utah, and Colorado: Professional Paper USGS Numbered Series 1506–E, http://pubs.er.usgs.gov/publication/pp1506E.
- Smith, M.E., Carroll, A.R., and Scott, J.J., 2015, Stratigraphic Expression of Climate, Tectonism, and Geomorphic Forcing in an Underfilled Lake Basin: Wilkins Peak Member of the Green River Formation, *in* Smith, M.E., and Carroll, A.R. (eds.), Stratigraphy and Paleolimnology of the Eocene Green River Formation, Western U.S.: Springer, 61-102.
- Smith, M.E., Carroll, A.R., and Singer, B.S., 2008, Synoptic reconstruction of a major ancient lake system: Eocene Green River Formation, western United States: Geological Society of America Bulletin, v. 120, p. 54–84, doi: 10.1130/B26073.1.
- Smith, M.E., Carroll, A.R., Scott, J.J., and Singer, B.S., 2014, Early Eocene carbon isotope excursions and landscape destabilization at eccentricity minima: Green River Formation of Wyoming: Earth and Planetary Science Letters, v. 403, p. 393–406, doi: 10.1016/j.epsl.2014.06.024.
- Smith, M.E., Chamberlain, K.R., Singer, B.S., and Carroll, A.R., 2010, Eocene clocks agree: Coeval 40Ar/39Ar, U-Pb, and astronomical ages from the Green River Formation: Geology, v. 38, p. 527–530, doi: 10.1130/G30630.1.
- Smoot, J.P., 1983, Depositional subenvironments in an arid closed basin; the Wilkins Peak Member of

- the Green River Formation (Eocene), Wyoming, U.S.A.: Sedimentology, v. 30, p. 801–827, doi: 10.1111/j.1365-3091.1983.tb00712.x.
- Stanfield, K.E., and Frost, I.C., 1949, Method of Assaying Oil Shale by a Modified Fischer Retort; U.S. Bureau of Mines, Report of Investigations 4477, 13 p.,
- Surdam, R.C., and Stanley, K.O., 1979, Lacustrine sedimentation during the culminating phase of Eocene Lake Gosiute, Wyoming (Green River Formation): Geological Society of America Bulletin, v. 90, p. 93–110, doi: 10.1130/0016-7606 (1979)90<93:LSDTCP>2.0.CO;2.
- Tranvik, L.J., and 31 other, 2009, Lakes and reservoirs as regulators of carbon cycling and climate: Limnology and Oceanography, v. 54, p. 2298–2314.
- Veizer, J., and 14 others, 1999, $^{87}\text{Sr}/^{86}\text{Sr}$, $\delta^{13}\text{C}$ and $\delta^{18}\text{O}$ evolution of Phanerozoic seawater: Chemical Geology, v. 161, p.59-88.
- Wiig, S.V., Grundy, W.D. and Dyni, J.R., 1995, Trona resources in the Green River Basin, southwest Wyoming. US Geological Survey Open-File Report OF 95-476.
- Zachos, J.C., Dickens, G.R., and Zeebe, R.E. (2008), An early Cenozoic perspective on greenhouse warming and carbon-cycle dynamics: Nature, v. 451, p. 279–283, doi: 10.1038/nature06588.